Spray quenching of specimen for ring heat treatment

P. Stark, S. Schuettenberg & U. Fritsching
Research Centre "Distortion Engineering",
Foundation Institute for Materials Science (IWT), Bremen, Germany

Abstract

The quenching process of metallic workpieces within manufacturing and heat treatment can be optimized by applying locally and temporally adapted quenching cooling conditions. Locally variable heat transfer conditions at the workpiece surface are realizable by the regulation of adjustable and flexible flow fields on the basis of impinging spray or jet flows. For the analysis of heat treatment, the heat transfer rates with respect to the applied flow parameters and their influence on the cooling conditions are described. The simulation is assisted by experimental analysis of impinging multiphase jets and sprays.
Keywords: spray cooling, quenching, heat treatment, heat transfer coefficient.

1 Introduction

A main step in the manufacturing process of e.g. machine and gear components is the heat transfer process. Large metallic rings are used in many technical applications. Due to their function as a main component of bearings high demands on material quality and precision are made during the production process. Large distortion and/or shape deviation occur during the process steps of heating, rolling and quenching that commonly require material allowance to enable an additional reworking process.

Thus, a new approach to minimize the occurring distortion has been developed in which the heat necessary for the forming process shall be used to compensate the distortion during quenching within the hardening process. The minimization and compensation of workpiece distortion can be realized by impressing asymmetric cooling conditions by the use of flexible flow fields based on liquid jets or sprays. Especially the cooling by two phase sprays of gas

WIT Transactions on Engineering Sciences, Vol 70, © 2011 WIT Press
www.witpress.com, ISSN 1743-3533 (on-line)
doi:10.2495/MPF110171

and liquid, as schematically showed in figure 1, enables to generate specific local heat transfer conditions on workpiece surfaces. The quenching process in flexible jet nozzle fields has originally been developed for gaseous flows [1]. But experimental investigations on relevant parts result in insufficient experiences because of the limited achievable heat transfer by this quenching method, which is too low for successful distortion compensation. However, by controlled quenching in liquid media (such as water or hardening oil) and by means of jet or spray quenching, the heat transfer process can be heavily intensified and to generate a much higher distortion compensation potential [2].

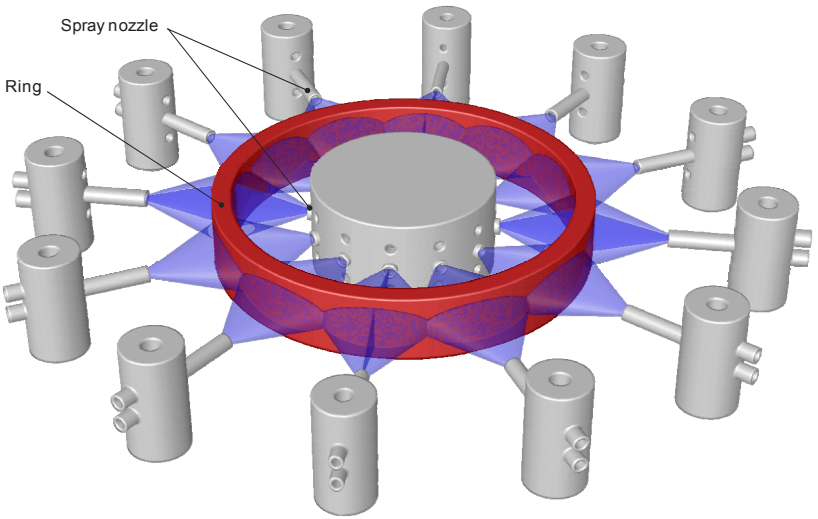

Figure 1: Spray quenching of heated rings.

In liquid jet quenching processes, the generated flow velocity on the impingement area outside a liquid jet should be strong enough to suppress any boiling phenomena (vapour layer, nucleate boiling) in the impingement region on the heated surface. Here, pure convective/single phase heat transfer from the workpiece surface to the incident flow will generate extremely high cooling rates and thus high heat transfer rates. For the numerical simulation these processes, Computational Fluid Dynamics (CFD) simulations are done. To achieve accurate results within the simulation of the heat transfer on the ring segment's surface, the complete flow field of the jet array could be rebuilt in a 3D-CFD-simulation. The chart of figure 2 shows the results of heat transfer coefficient (HTC) allocations along a vertical scanline through the centres of impinging jets on a heated ring segment surface. It can clearly be seen that the impinging liquid jet causes significant higher HTC-profiles ($\alpha_M \approx 25$ kW/(m²K)) in comparison to the results of the gas quenching process ($\alpha_M \approx 1$ kW/(m²K)). The high level of the local HTC shows the high distortion compensation potential of the liquid jet quenching process. However, quenching experiments showed that the impressed local HTC are too high for a useful control of asymmetric quenching conditions.

In consequence, two-phase atomizers instead of single-phase liquid jets are utilized to allow the adjustment of impressed heat transfer conditions with the choice of spray parameters (liquid mass flow and gaseous pressure). This quenching technique enables to set up local heat transfer conditions to generate HTC results in a useful range between the achievable results for pure gas respectively liquid quenching processes, as shown in figure 2.

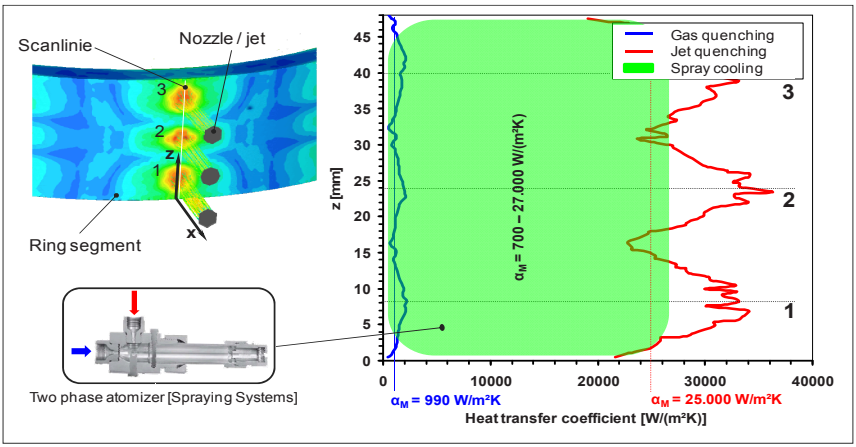

Figure 2: Heat transfer coefficients for different jet and spray cooling techniques.

Through the use of multiphase atomizers for impressing intensive but controlled local heat transfer on surfaces, it is also possible to avoid vapour layer formation on heated workpiece surfaces [3, 4]. A spray of fine liquid droplets and an overlaid gaseous flow is impinged on the heated surface. Within this process, the efficiency of a complete evaporative cooling should be ideally reached, because the liquid fraction of the spray is restricted so that no closed liquid film with a vapour layer underneath is built.

For experimental investigations on hot rings, a flexible nozzle field shall be utilized to create local gradients in heat transfer, so that the occurring internal stresses lead to a compensation of the distortion while the surface hardness is not dropping below given requirements. To detect and compare the occurring distortion of the quenched parts, the shape deviations of the specimens with respect to the applied quenching conditions are measured through a mechanical measuring system before and after the cooling process.

2 Methods

2.1 Experimental setup

To analyse the spray cooling process, a twin fluid atomizer with water and air is used. This nozzle (type: CasterJet, manufacturer: Spraying Systems Co.) is typically applied for cooling in steel casting processes and is assigned by very

high mass fluxes (up to 1600 kg/h) for the liquid phase. The spray pattern of this atomizer type is a flat-spray cone, which is the optimal geometry for a homogeneous cooling over the circumference of the given ring segment. A spray pattern at typical operation parameters (water mass flow 100 kg/h, air pressure p = 0.3 MPa) and position related to a workpiece surface is shown in figure 3. The given operation parameters (air pressure and water mass flow) and especially the operation boundaries are examined and defined in experimental investigations.

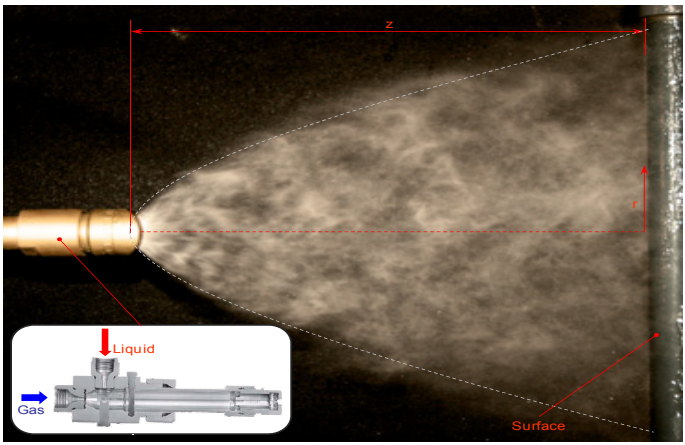

Figure 3: Two phase atomizer arrangement for spray cooling.

For efficient estimation of the spray process, a spray characterization in combination with evaluation and cooling curve based measurements of heat transfer coefficients are performed. The spray characterization consists of drop diameter measurements by using Laser Diffraction Techniques and droplet velocity examinations done by Particle Image Velocimetry (PIV). The measurement of liquid mass flux distributions is done by using patternators.

The cooling behaviour of 1/16 segments of a large ring (figure 4) with respect to the applied spray quenching conditions is investigated experimentally. Both inside and outside of the ring two spray nozzles are arranged perpendicularly to the surface, so that the flat spray profile is only widening in the circumferential direction. The area of impingement is located at half of the ring's height. A constant nozzle distant of z = 140 mm provides an overlapping region of about 30% of the width of one single spray cone on both sides of the ring segment. The ring segment is heated for 90 minutes at T_{oven} = 900°C under ambient atmosphere. The spray nozzles were activated at t = 0 s as soon when the specimen is reaching the desired position in the nozzle field. During quenching, the temperature at different positions inside of the specimen have been measured through thermocouples (NiCr-Ni, Type K), both in the core (diameter = 1 mm) and in the near-wall region (diameter = 0.5 mm). The distances from the surface of the near-wall thermocouples are in the range of 1 - 1.5 mm. The measurement frequency is 15 Hz.

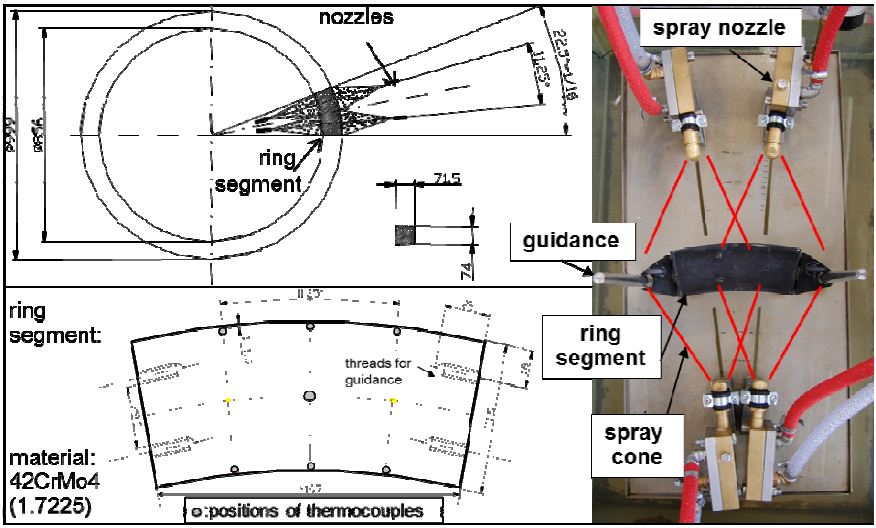

Figure 4: Experimental setup for quenching of ring segment with sprays.

2.2 Determination of heat transfer coefficients

The basis for high heat transfer rates in spray cooling processes is a high evaporation efficiency. It increases for decreasing drop diameters and is often used in dependency to the Weber number, whereby the drop behaviour during workpiece surface impact can be characterized and evaluated by approaches of Bolle and Moureau [5] and Berg [6]:

$$We = \frac{u^2 \cdot \rho \cdot d}{\sigma} \tag{1}$$

Here, u is the drop velocity [m/s], ρ is the density of the liquid phase [kg/m^3], d is the drop diameter [m] and σ the surface tension [N/m]. For Weber numbers above 80, a liquid film is built on the heated surface. The film next collapses in a number of small drops which results in a high heat transfer. For setting up high evaporation efficiency, it is necessary to adjust the spray for getting Weber numbers above 80.

For evaluation of heat transfer coefficients, the empiric approach of Puschmann [3] was the chosen:

$$\alpha_C = \dot{m}_S \cdot 16{,}8 \cdot u^{0.12} \cdot d^{-0.29} \tag{2}$$

Here, α_c is the convective heat transfer coefficient [W/(m^{2}K)] and m_s is the impingement density [kg/(m^{2}s)]. Puschmann could show that the results for calculated heat transfer coefficients in spray cooling processes are directly proportional to the water impingement density for heated surfaces above the Leidenfrost temperature. The drop diameter and velocity only have a secondary role in comparison to the water impingement density.

Based on measured temperature curves at the near-wall thermocouples, the underlying time-dependent heat transfer coefficient (HTC) on the surface can be determined by applying a numerical approach. It is based on the observation that the temperature in the near-wall region is decreasing rapidly, while the reaction of the temperature in the core is heavily delayed due to the thickness and the relatively low thermal conductivity of the solid (Biot number Bi > 1). By also neglecting cross flows of energy in the axial direction of the ring, each of the measurement positions is treated individually as a one-dimensional stripe of the solid with the length $(r_{outer} - r_{inner})/2$ involving the core and the very tip of the thermocouples.

In this approach, energy can only be removed through that boundary representing the outer surface of the specimen. All other walls are set to adiabatic. Starting from a homogenous temperature distribution of $T = T_{oven}$, the heat transfer coefficient on the surface is iteratively calculated for each time step until the simulated temperature at the position of the thermocouple corresponds to that one from the experiment within a $\pm$ 0.1°C interval. Within this loop, the current temperature distribution at time t is used as the initial condition to determine the heat transfer coefficient at time $t + \Delta t$.

This approach enables to calculate the time-dependent heat transfer coefficient at the wall for all cooling curves at the beginning of the quenching process. For a two-sided flat plate with the thickness d cooled from both sides, it is valid for [7]:

$$Fo = \frac{a \cdot t}{(d/2)^2} \leq 0.04 \tag{3}$$

Here, the Fourier number Fo is calculated with the thermal diffusivity a [m^2/s] of the steel, the time t and the characteristic length d. Setting $d = (r_{outer} - r_{inner})$ leads to a validity period of $t \leq 28$ s for the ring segment.

2.3 Numerical simulation of the temperature distributions

The determined time-dependent heat transfer coefficients can be used as a boundary condition for the simulation of the cooling of the specimen. Due to the limited number of thermocouple measurements, these values are linearly interpolated in circumferential direction between these known locations at each time step. In axial direction, no gradient in heat transfer is applied. At the other surfaces (upper, lower and end faces) which are not directly exposed to an incoming flow, low values for the heat transfer coefficients of 2000 W / (m^2K) are assumed and kept constant for the entire calculation. Starting from a homogenous temperature distribution of 900°C, the cooling until equilibrium ($T_{ambient}$ = 25°C) is simulated. Temperature dependent material properties of the material (42CrMo4) are applied during the calculation of the unsteady cooling of the specimen.

3 Results

3.1 Heat transfer coefficients based on cooling curves

The cooling behaviour at different position in the ring segment has been measured for a symmetric and an asymmetric nozzle setup at different positions inside of the specimen (see figure 5):

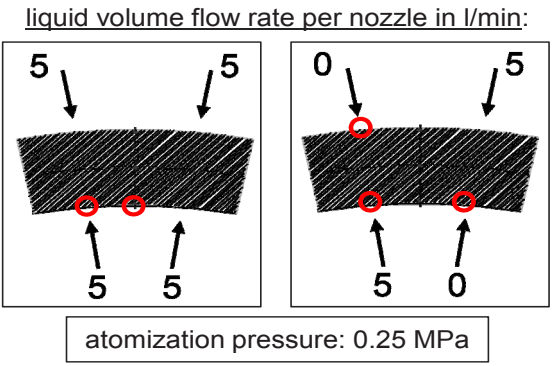

Figure 5: Symmetric (l.) and asymmetric spray nozzle setup, positions of the thermocouple measurements.

The cooling curves measured in the centre of a spray cone show the same result regardless whether the symmetric or asymmetric respectively the convex or concave surface is analysed. Thus, they are used as the reference curve in figure 6, in which the measured cooling curves are compared.

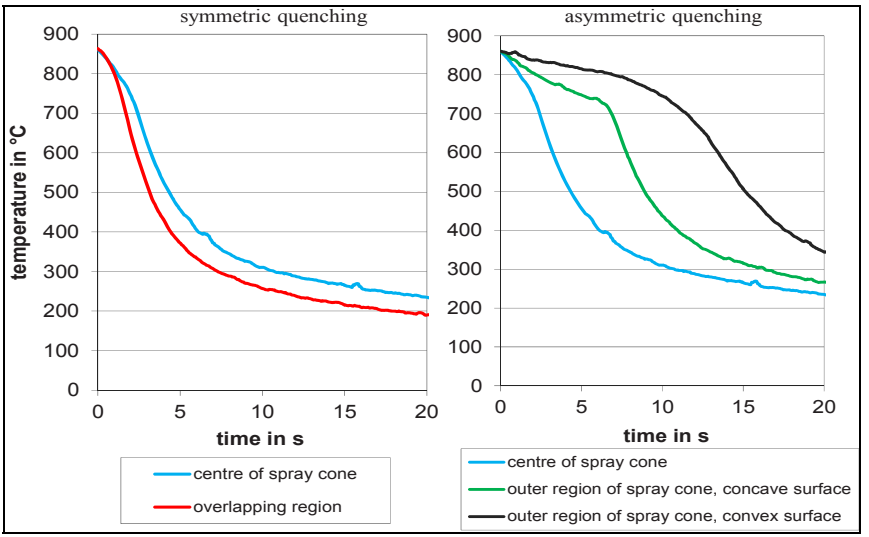

Figure 6: Measured cooling curves for spray quenching.

At symmetric quenching conditions, the cooling behaviour is qualitatively the same at both measuring position, but a slightly faster temperature decrease can be observed in the overlapping region.

In case of asymmetric quenching conditions, the cooling behaviour in the outer regions of the spray cones follows a differing trend. On both sides of the ring segment, a period of only slow temperature decrease may be observed within the first few seconds of the quenching process followed by a more abrupt decrease of the temperature, which is typical for occurring boiling phenomena.

Due to the geometric shape of the surfaces this trend is more emphasized on the outer side of the specimen. There, the convex surface shape leads to a more acute angle of impingement of the spray, so that the stagnation pressure of the flow may not be high enough to transport away any formed vapour film. After the collapse of the vapour film, the cooling trend is very similar at all measurement positions.

The corresponding cooling trends in the core regions down to a temperature of 400°C are not differing significantly. It takes 82 s in case of symmetric quenching conditions, whereas 95 s are necessary when the asymmetric quenching conditions are applied.

The heat transfer coefficient has been determined by applying the numerical approach described in chapter 2.2. The results are summarized in figure 7.

For almost all curves, the heat transfer coefficient increases rapidly at the beginning of the quenching process increases, until it stays at a constant level. For the symmetric quenching conditions, this constant region is reached after

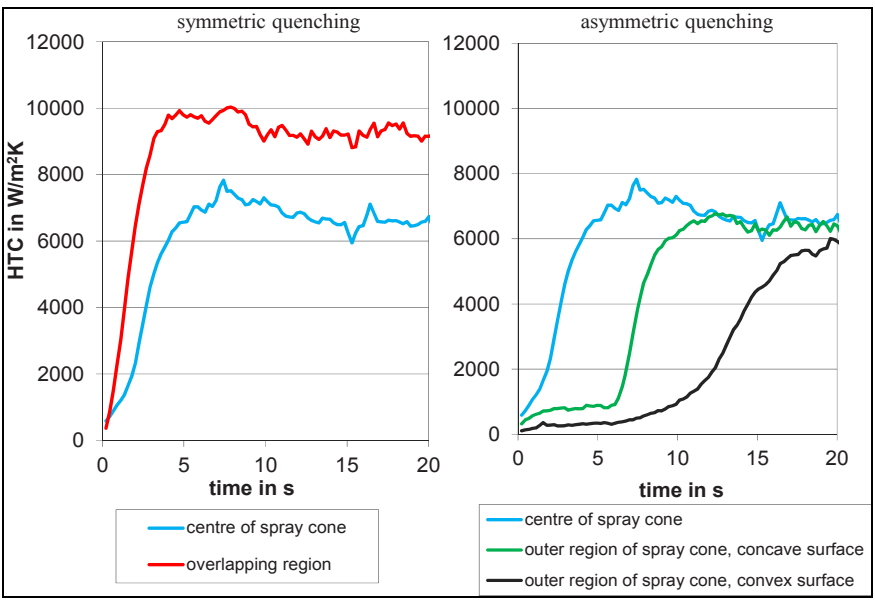

Figure 7: Determined time-dependent heat transfer coefficient for spray quenching.

about the same period of time (≈ 4 s) both in the core region of the spray cone as well as an in the overlapping region. In the overlapping region, this constant HTC has a value of about 9100 W / (m²K) compared to 6700 W / (m²K) in the centres of the single spray cones.

For the asymmetric quenching conditions, the reached constant value of 6700 W / (m²K) is almost equal at all measured location, but the described effect of the boiling phenomena on the hot surface in the outer regions of the spray cones leads to a time shift of about 5 s between the three measurement positions, concerning the point in time when the low HTC ≤ 2000 W / (m²K) are quickly increases to the higher values in the constant regime of the HTC.

3.2 Heat transfer coefficients based on calculation approach validation

The CasterJet nozzle was used for measurements by different water mass flows and air pressures. The result of the drop diameter measurements on the spray axis for a distance of z = 140 mm is shown in the left charts of figure 8 in dependence of the mean volumetric diameter d_{30} with the water mass flow and air pressure. It can be seen that the d_{30} increases with increasing water mass flow, but it shrinks in proportion to increased air pressures.

The local drop velocities inside the spray were measured by the use of PIV method. The right charts of figure 8 shows exemplarily results of velocity measurements for typical water mass flows by air pressure 0.15 MPa. The trend of the averaged velocities for an increased distance to the spray axis shows a maximum on position r = 0 and a light decrease of the velocity for outer ranges.

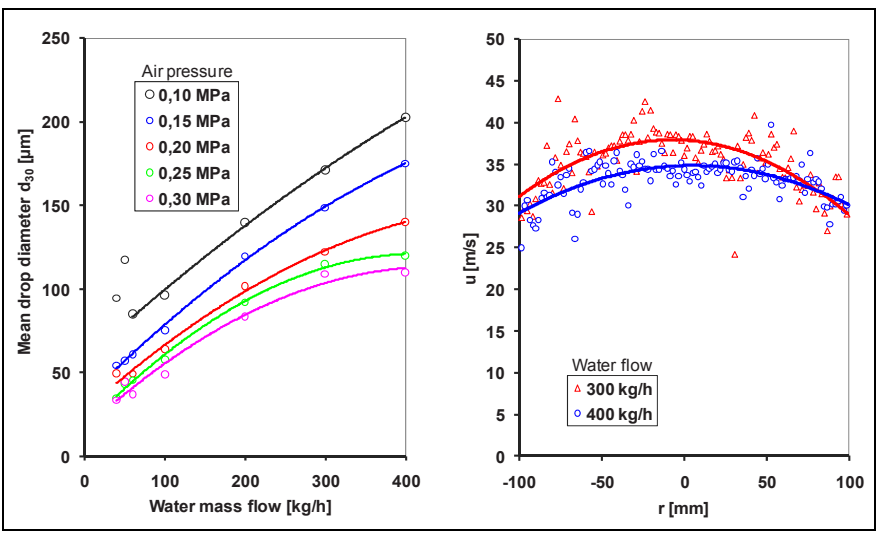

Figure 8: Measured mean drop diameter (l.) and drop velocity dependent to spray parameters.

With knowledge of the drop diameter and velocities on different points inside the spray it is possible to calculate local Weber numbers by eqn (1). The calculated Weber numbers should validate the applicability of the used approach for calculating local heat transfer coefficients by eqn (2). The calculations result in Weber numbers higher than 85 for every spray parameter combination (water mass flow and air pressure). Based on this, eqn (2) is valid.

By [3] the calculated heat transfer coefficients are direct proportional to the water impingement density. The impingement density was measured on different positions inside the spray for the distance of z = 140 mm. Figure 9 shows results on the dependence of the water mass flow and used air pressures.

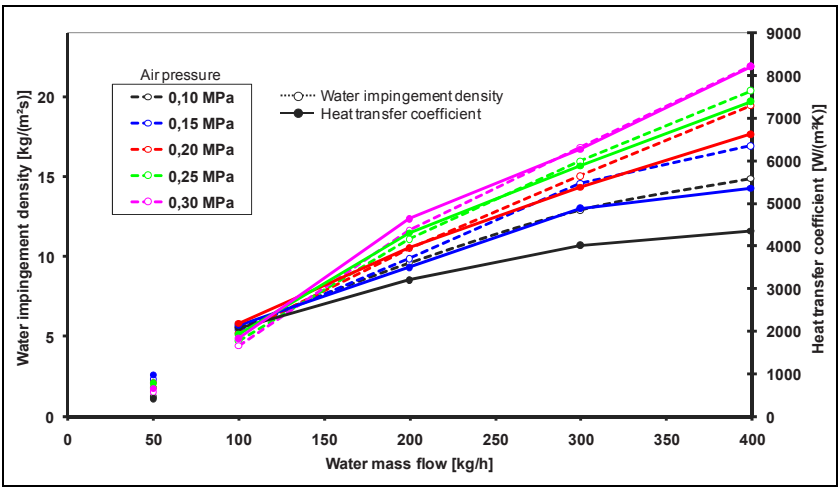

Figure 9: Heat transfer coefficients and water impingement density.

The determined results from the spray characterization for drop diameter, velocities and impingement densities are used to calculate heat transfer coefficients by eqn (2) for the position r = 0. The results of these calculations are also included in figure 9 for direct comparison. Based on this, a direct proportionality of the water impingement density to the heat transfer coefficients can be validated under consideration of the adjusted air pressures.

3.3 Temperature distributions in ring during quenching

The temperature distributions inside of the ring segments are calculated by using the determined local heat transfer coefficients as the boundary condition in the numerical simulation (see figure 10).

For symmetric and asymmetric quenching conditions, the temperature distributions are shown at a certain time step, so that the maximum temperature in the core region is 400°C. The corresponding cooling process takes 75 s in case of symmetric quenching with four activated spray nozzles, resp. 90 s for the asymmetric quenching conditions with only two used nozzles (compare to

chapter 3.1). A response of the temperature distribution to the applied quenching intensities can still be observed both in the core and in the near-wall regions of the specimen. An additional comparison of the experimentally and numerically determined cooling curves in the core regions shows good agreements within a ±30°C interval.

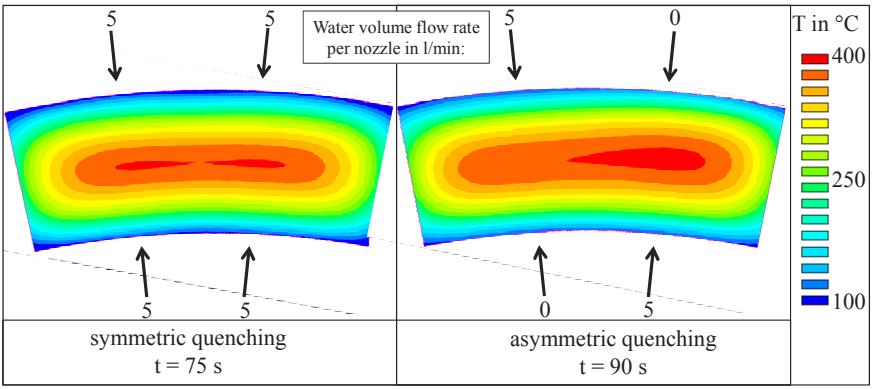

Figure 10: Simulated temperature distributions at cutting planes through the centres of the ring segments (atomization pressure p = 0.25 MPa).

4 Conclusion

By creating asymmetric quenching intensities on the specimen's surface, local gradients in the internal cooling behaviour inside of the body can be caused which may lead to increased distortion behaviour of the quenched specimens.

The general merits of the spray quenching technique and the influence of the spray parameters on the local cooling conditions were presented. The decisive precondition for this approach is the knowledge of the local spray conditions and their influence on the temporal and spatial distribution of the heat transfer rates. Here, two different approaches to determine the heat transfer coefficient were shown.

The effect of the temperature distributions and local cooling rates during quenching of a ring is demonstrated.

Acknowledgement

The present work was executed in the framework of the Collaborative Research Centre (SFB 570) "Distortion Engineering" at the University of Bremen (projects B4 and T5). The authors would like to thank the German Research Foundation (DFG) for the financial support.

References

[1] Schuettenberg, S., Frerichs, F., Hunkel, M., Fritsching, U., Int. J. Materials and Product Technology; 24, 2005, 259-269
[2] Schüttenberg, S., Hunkel, M., Fritsching, U., Zoch, H.-W., Proc. of 5th International and European Conference on Quenching and Control of Distortion, 25 - 27 April 2007, Berlin, S. 257-264
[3] Puschmann, F.: "Experimentelle Untersuchung der Spraykühlung zur Qualitätsverbesserung durch definierte Einstellung des Wärmeübergangs", Dissertation, 2003, Otto-von Guericke-Universität, Magdeburg, Germany
[4] Krause, C., Wulf, E., Nürnberger, F., Bach, F.-W., Forsch. Ingenieurwes. 2008, 72, 163-173
[5] Bolle, L., Moureau, J.C., Multiphase Sci. Technol. 1982, 1, 1-97
[6] Berg, M., "Zum Aufprall, zur Ausbreitung und Zerteilung von Schmelzetropfen aus reinen Metallen", Dissertation, 1999, Universität Bremen, Germany
[7] Verein Deutscher Ingenieure: VDI-Wärmeatlas, 9. Auflage, Springer-Verlag Berlin (u.a.), 2002